Optical Properties of Mn-Doped CuGa(In)S-ZnS Nanocrystals (NCs)

Subjects: Engineering, Biomedical

Contributor: Xiaoshan Zhu ,

Mn-doped binary NCs have average fluorescence lifetimes in the range of sub-milliseconds and/or need high energy for excitation, or they contain the toxic elements of Cd and/or Se against biosensing/imaging applications.

time-gated fluorescence measurement Mn doping

1. Introduction

Mn-doped NCs, once the exciton energy is transferred to the $^4T_1$ state of the Mn dopants, the spin relaxation and slow inversion between the $^4T_1$ and $^6A_1$ states of Mn should cause an ideal yellow emission at ~585 nm with a long lifetime [1]. Mn elements have been doped into different types of NCs including binary NCs (e.g., CdSe or ZnSe NCs) or multinary NCs (e.g., I(II)-III-VI NCs) [1][2][3][4][5][6][7][8][9][10]. When Mn is doped into binary excitonic NCs, the excitonic fluorescence of host NCs will be completely quenched and only the Mn emission should emerge, because the transfer of the exciton energy to the Mn $^4T_1$ state is much faster compared to the excitonic recombination of host NCs [2][3][4][5][6][7][8][9][10]. With respect to their optical properties, the absorption spectra of Mn-doped binary excitonic NCs are still determined by the bandgap of these host NCs, but the fluorescence brightness and lifetime of the doped NCs will be mainly affected by the Mn–Mn interaction in these host NCs [9][10]. Generally, Mn-doped binary NCs have average fluorescence lifetimes in the range of sub-milliseconds and need high energy for excitation, or they contain the toxic elements of Cd and/or Se against biosensing/imaging applications.

Among many multinary NCs, I(II)-III-VI NCs such as Cu-In-S/ZnS and Cu-Zn-In-S/ZnS NCs do not contain any Cd or Se elements and are particularly attractive to biomedical applications [11][12][13][14][15]. Different from binary excitonic NCs, they are donor–acceptor-pair-model-based materials. In these NCs, the donor states could be attributed to sulfur vacancies, silver/copper interstitials and gallium/indium atoms occupying substituted silver/copper sites, and the acceptor states could be from indium/gallium interstitials and silver/copper atoms occupying gallium/indium sites [11][12][13][14][15][16][17]. The fluorescence of I(II)-III-VI NCs should be mainly attributed to the electron transition from the donor states to acceptor states [11][12][13][14][15][16][17][18]. Moreover, the optical properties of I(II)-III-VI NCs can be adjusted by diverse compositional combinations among monovalent copper/silver and trivalent indium/gallium, as well as further monovalent-to-trivalent cation stoichiometric variation [19]. For Mn-doped I(II)-III-VI NCs, upon photoexcitation, the excitation energy of the host I(II)-III-VI NCs can be transferred to both Mn dopants and donor states, which could result in both Mn emission and donor–acceptor emission, or the dominant Mn emission. Additionally, the microenvironments (e.g., defects, electronic structures) in the I(II)-III-VI host NCs, which are determined by compositional combination and element stoichiometric variation in

NCs, would significantly affect the lifetime of the Mn emission [1][20]. Considering all these factors, the optical properties (fluorescence/absorption spectra, brightness and lifetimes) of Mn-doped I(II)-III-VI NCs would be versatile but also complex. For instance, some works on Mn-doped I(II)-III-VI NCs have been reported, but on the basis of their own particular synthetic approaches, they presented significant changes in fluorescence lifetimes (hundreds of nanoseconds to milliseconds) and fluorescence wavelengths (yellow to red), presented complex steps in synthesis, or still needed high energy (UV light) for NC excitation due to the adoption of wide-bandgap NCs [21][22][23][24][25]. Some studies intended to synthesize NCs with double emission peaks from both Mn emission and donor–acceptor emission for photovoltaic applications (e.g., white LEDs) [26][27][28][29].

Specific to the applications in time-gated measurements, more efforts are still needed to investigate Mn-doped I(II)-III-VI NCs towards achieving the desired features (high brightness, low-energy excitation, and long lifetimes up to milliseconds) as time-gated probes.

2. Effects of Host NC

From **Figure 1**A, it can be seen that the host NCs (without Mn doping) have peak emissions at around 500 nm, 530 nm, 545 nm and 570 nm, respectively. The QYs of all host NCs are low in the range of 0.5% to 5%, which indicate significant defects in all the prepared host NCs. As the Mn dopants are incorporated into each type of host NCs to form Mn-doped NCs, it can be seen that no matter which type of host NC is adopted, all of the Mn:CuGaS-ZnS and Mn:CuInS-ZnS NCs present almost the same emission spectra (**Figure 1**A). All the emission peaks are around 595 nm and all the emission spectra present almost the same shape profiles and the same FWHMs at around 60 nm. With respect to emission brightness, the QY is 47% for Mn:CuGaS-ZnS (Cu/Ga = 1/8) NCs, 12% for Mn:CuGaS-ZnS (Cu/Ga = 1/4) NCs, 14% for Mn:CuInS-ZnS (Cu/Ga = 1/8) NCs, and 3% for Mn:CuInS-ZnS (Cu/Ga = 1/4) NCs. Mn-doped NCs are significantly brighter than the corresponding host NCs. For host CuGaS-ZnS NCs with both Cu/Ga = 1/8 and Cu/Ga = 1/4, before and after Mn doping, their absorption spectra are almost similar. This indicates that Mn doping into these host NCs is not significantly affecting the bandgaps of the host NCs.

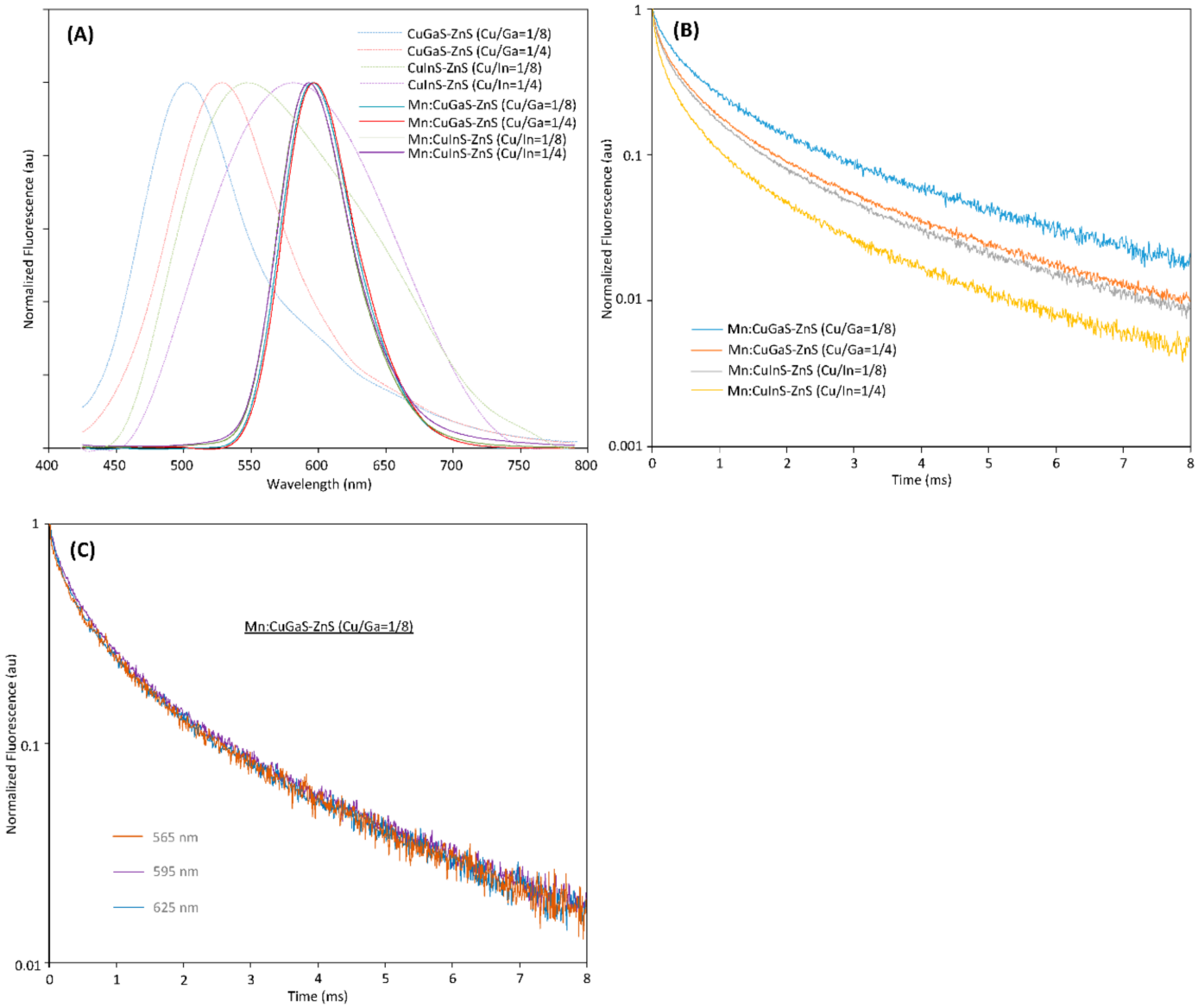

Figure 1. (**A**) Fluorescence spectra of four types of host NCs and four types of Mn-doped NCs (0.0125 mmol Mn-doped into each type of host NCs). (**B**) Fluorescence decays for four types of Mn-doped NCs (measured at 595 nm for all NC samples). (**C**) Fluorescence decays of Mn:CuGaS-ZnS (Cu/Ga = 1/8) NCs at 565, 595 and 625 nm.

3. Effects of Mn Concentration in NCs

With respect to brightness (QY), lifetime, and low energy for excitation (excitable by visible light at 405 nm), Mn:CuGaS-ZnS (Cu/Ga = 1/8) NCs are optimal and have potential to be further developed as time-gated probes for TGFM, and thus the effects of Mn concentration on this type of host NC were further investigated.

Figure 2A shows the emission-absorption spectra of Mn:CuGaS-ZnS (Cu/Ga = 1/8) NCs with different Mn concentrations in synthesis. The emission spectra of all Mn-doped NCs present almost the same emission spectra. All emission peaks are around 595 nm except that of Mn = 0.05 mmol at around 600 nm. All emission spectra present almost the same shape profiles and the same FWHMs at around 60 nm. For the emission spectra of the

NCs that used Mn = 0.00312 and 0.00625 mmol in their synthesis, a tail is observed in the range of 450–510 nm. It is believed that due to the limited Mn dopants in the synthesis, not all the donor–acceptor emissions are quenched, and a small amount of light is still from the donor–acceptor emissions [26][27][28].

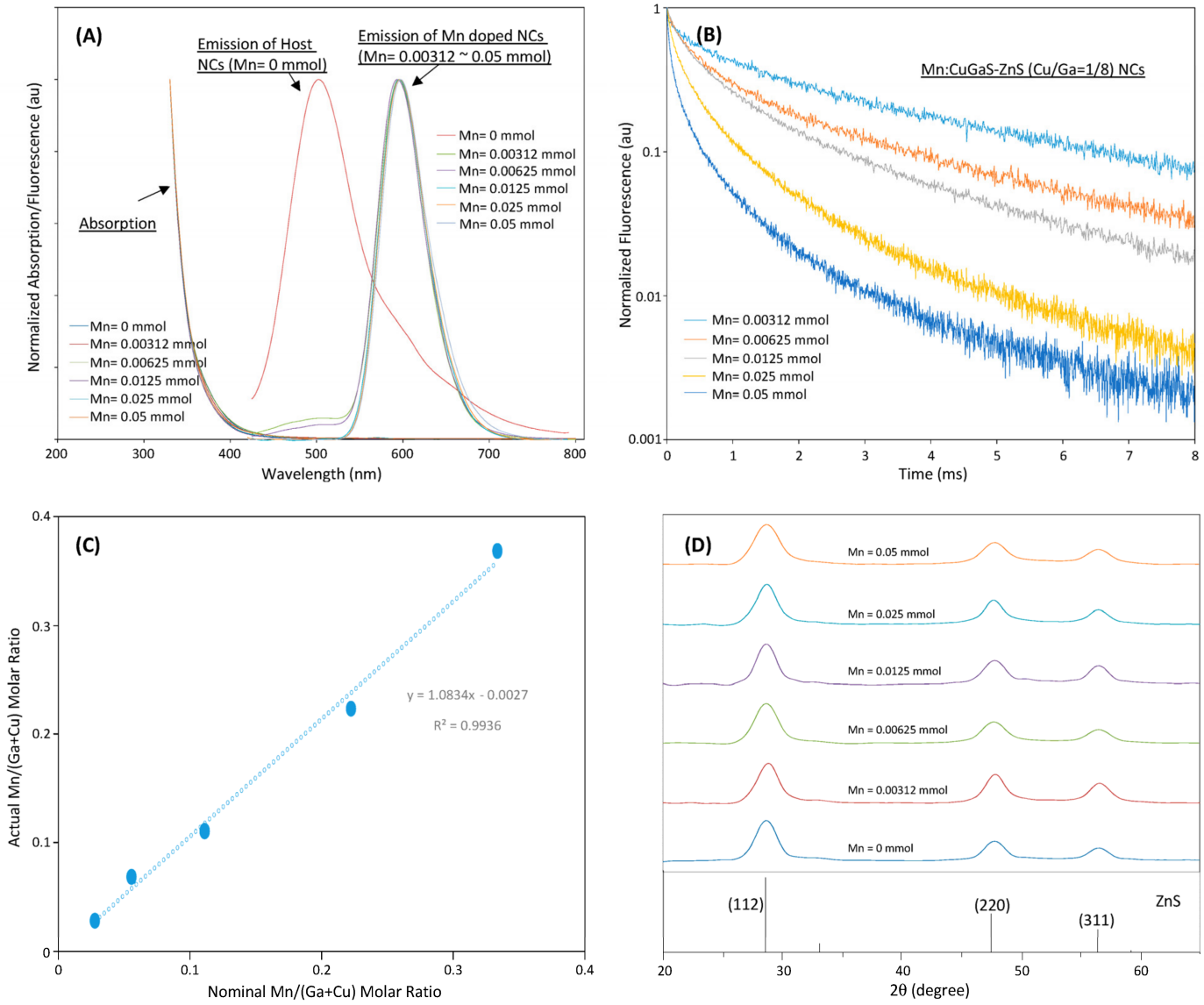

Figure 2. (**A**) Fluorescence and absorption spectra of CuGaS-ZnS (Cu/Ga = 1/8) NCs and Mn:CuGaS-ZnS (Cu/Ga = 1/8) NCs with a wide Mn-concentration range in synthesis. (**B**) Fluorescence decays of Mn:CuGaS-ZnS (Cu/Ga = 1/8) NCs at their peak wavelengths with different Mn concentrations in synthesis. (**C**) ICP-based actual Mn/(Ga + Cu) molar ratios of Mn:CuGaS-ZnS (Cu/Ga =1/8) NCs with a series of Mn concentrations in synthesis. (**D**) XRD patterns of Mn:CuGaS-ZnS (Cu/Ga = 1/8, Mn = 0.0125 mmol) NCs with different Mn concentrations in synthesis.

4. Demonstration of Time-Domain Fluorescence Characteristics under Pulsed 405 nm Laser Excitation and Bandpass-Filter-Based Emission Collection

In most applications of TGFM, probes with a long fluorescence lifetime are often excited using a light source (e.g., laser diode) and their fluorescence signals are collected by photosensor (such as PMT) through a bandpass filter. To demonstrate the potential of the Mn-doped NCs as probes for practical TGFM applications, researchers built an optical-measurement system to measure the time-domain fluorescence characteristics of Mn-doped NCs, as illustrated in **Figure 3**A. In this demonstration, the host CuGaS-ZnS (Cu/Ga = 1/8) NCs and Mn-doped CuGaS-ZnS (Cu/Ga = 1/8, Mn = 0.003215, 0.0125, 0.05 mmol) NCs were selected. **Figure 3**B shows the normalized system responses from all the selected NCs (suspended in chloroform) within a period of laser pulse. It is clear that after the laser turns off, the fluorescence signal of the host NCs without Mn doping drops off very fast (due to their lifetime of several hundreds of nanoseconds), but other Mn-doped NCs present long fluorescence decays (due to lifetimes at around 1 ms or longer). As Mn concentration is increased from 0.003125 to 0.0125 to 0.05 mmol, the Mn-doped NCs present the slowest decay to the fastest decay, which matches the change trend of the measured lifetime vs. the change in Mn concentration. This demonstration clearly indicates that the fluorescence decay of Mn-doped NCs would make it feasible for time-gated instruments to capture fluorescence signals after the laser is off [30]. On the other hand, since NC-surface-modification approaches for phase transfer and bioconjugation are well-established [31], these surface-modification approaches are readily applicable to these Mn-doped NCs for broad time-gated biosensing/imaging applications.

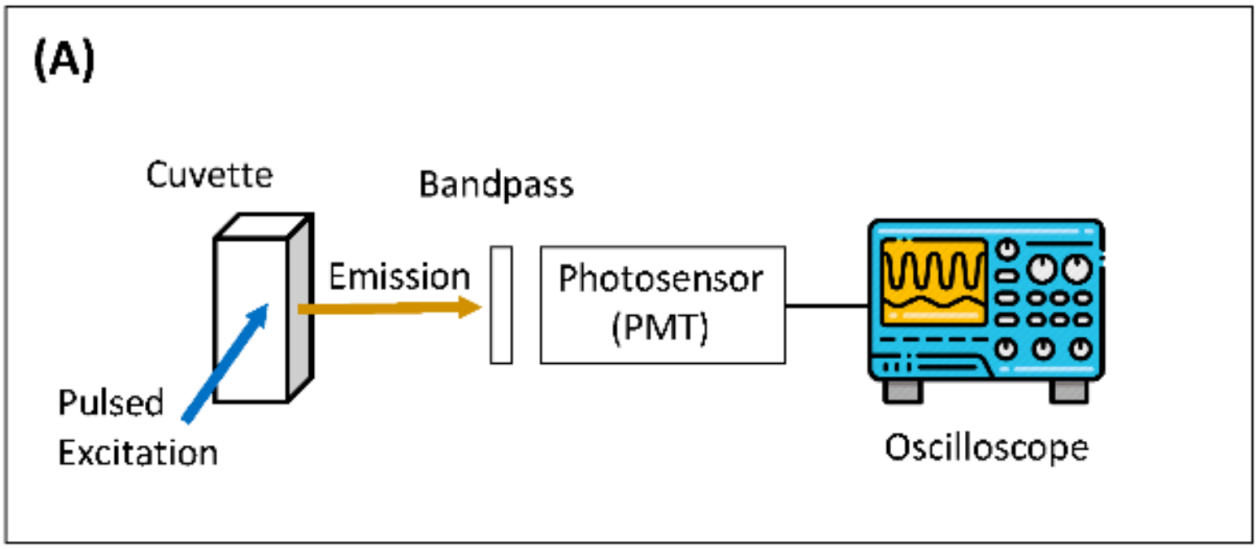
(A)
Cuvette
Bandpass
Emission
Photosensor
(PMT)
Pulsed
Excitation
Oscilloscope

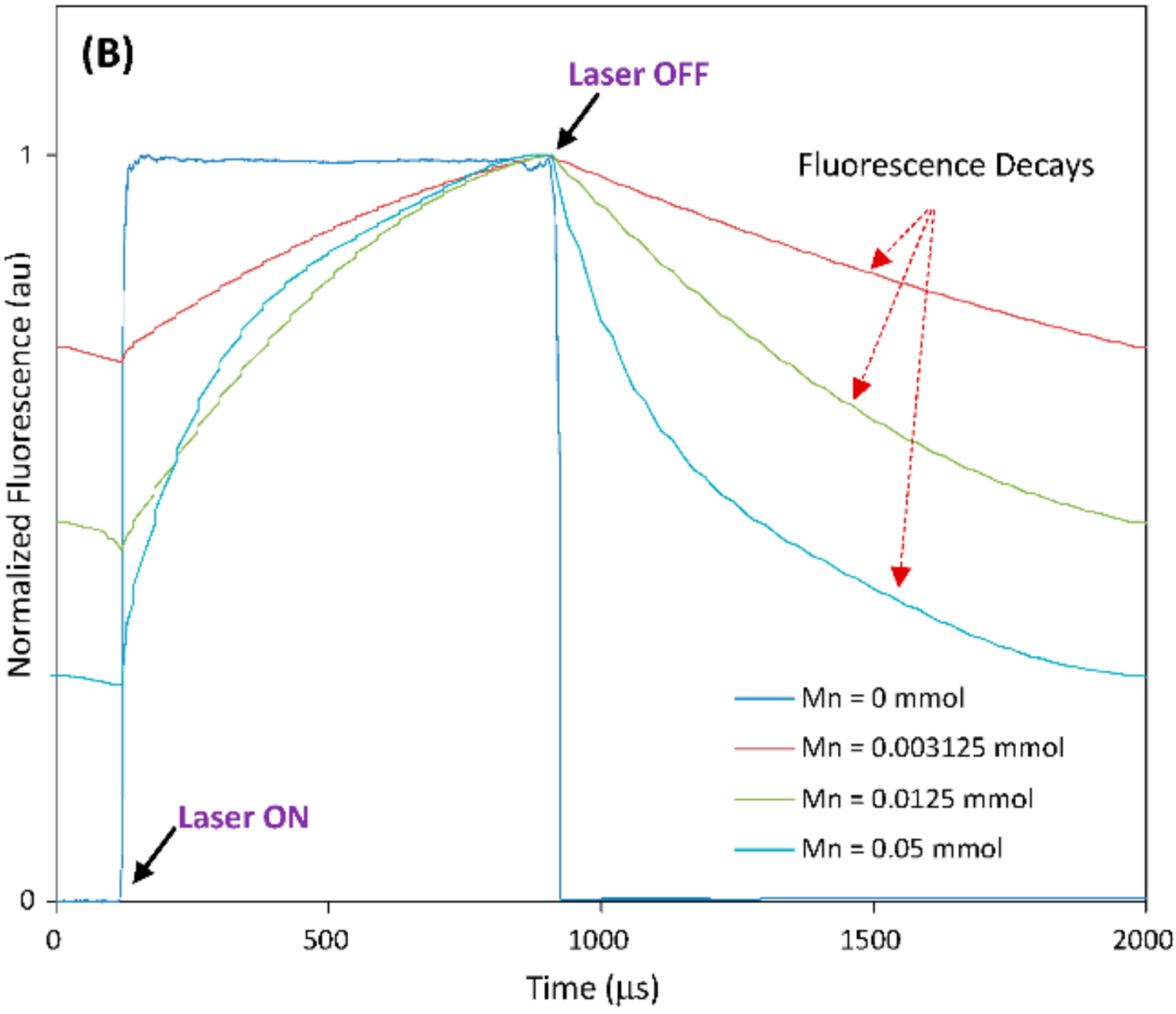
(B)
Laser OFF
Fluorescence Decays
Laser ON
Mn = 0 mmol
Mn = 0.003125 mmol
Mn = 0.0125 mmol
Mn = 0.05 mmol
Normalized Fluorescence (au)
Time (µs)
0
1
0
500
1000
1500
2000

Figure 3. (**A**) The setup illustration of the optical-measurement system. (**B**) The normalized system responses from all selected NCs within a period of laser pulse (host CuGaS-ZnS with Cu/Ga = 1/8, and Mn-doped CuGaS-ZnS with Cu/Ga = 1/8 and Mn = 0.003215, 0.0125, 0.05 mmol, respectively).

References

1. Pradhan, N. Mn-Doped Semiconductor Nanocrystals: 25 Years and Beyond. J. Phys. Chem. Lett. 2019, 10, 2574–2577.
2. Karan, N.S.; Sarma, D.D.; Kadam, R.M.; Pradhan, N. Doping Transition Metal (Mn or Cu) Ions in Semiconductor Nanocrystals. J. Phys. Chem. Lett. 2010, 1, 2863–2866.
3. Zheng, J.; Ji, W.; Wang, X.; Ikezawa, M.; Jing, P.; Liu, X.; Li, H.; Zhao, J.; Masumoto, Y. Improved Photoluminescence of MnS/ZnS Core/Shell Nanocrystals by Controlling Diffusion of Mn Ions into the ZnS Shell. J. Phys. Chem. C 2010, 114, 15331–15336.
4. Zeng, R.; Rutherford, M.; Xie, R.; Zou, B.; Peng, X. Synthesis of Highly Emissive Mn-Doped ZnSe Nanocrystals without Pyrophoric Reagents. Chem. Mater. 2010, 22, 2107–2113.
5. Zheng, J.; Yuan, X.; Ikezawa, M.; Jing, P.; Liu, X.; Zheng, Z.; Kong, X.; Zhao, J.; Masumoto, Y. Efficient Photoluminescence of Mn2+ Ions in MnS/ZnS Core/Shell Quantum Dots. J. Phys. Chem. C 2009, 113, 16969–16974.
6. Zhang, W.; Li, Y.; Zhang, H.; Zhou, X.; Zhong, X. Facile Synthesis of Highly Luminescent Mn-Doped ZnS Nanocrystals. Inorg. Chem. 2011, 50, 10432–10438.
7. Suyver, J.F.; Wuister, S.F.; Kelly, J.J.; Meijerink, A. Luminescence of Nanocrystalline ZnSe: Mn2+. Phys. Chem. Phys. 2000, 2, 5445–5448.
8. Jindal, Z.; Verma, N.K. Photoluminescent properties of ZnS:Mn nanoparticles with in-built surfactant. J. Mater. Sci. 2008, 43, 6539–6545.
9. Hazarika, A.; Layek, A.; De, S.; Nag, A.; Debnath, S.; Mahadevan, P.; Chowdhury, A.; Sarma, D.D. Ultranarrow and Widely TunableMn2+-Induced Photoluminescence from Single Mn-Doped Nanocrystals of ZnS-CdS Alloys. Phys. Rev. Lett. 2013, 110, 267401.
10. Pu, C.; Ma, J.; Qin, H.; Yan, M.; Fu, T.; Niu, Y.; Yang, X.; Huang, Y.; Zhao, F.; Peng, X. Doped Semiconductor-Nanocrystal Emitters with Optimal Photoluminescence Decay Dynamics in Microsecond to Millisecond Range: Synthesis and Applications. ACS Cent. Sci. 2016, 2, 32–39.
11. Zhong, H.; Bai, Z.; Zou, B. Tuning the Luminescence Properties of Colloidal I–III–VI Semiconductor Nanocrystals for Optoelectronics and Biotechnology Applications. J. Phys. Chem. Lett. 2012, 3, 3167–3175.

12. Yarema, O.; Bozyigit, D.; Rousseau, I.; Nowack, L.; Yarema, M.; Heiss, W.; Wood, V. Highly Luminescent, Size- and Shape-Tunable Copper Indium Selenide Based Colloidal Nanocrystals. Chem. Mater. 2013, 25, 3753–3757.
13. Yoon, S.-Y.; Kim, J.-H.; Jang, E.-P.; Lee, S.-H.; Jo, D.-Y.; Kim, Y.; Do, Y.R.; Yang, H. Systematic and Extensive Emission Tuning of Highly Efficient Cu–In–S-Based Quantum Dots from Visible to Near Infrared. Chem. Mater. 2019, 31, 2627–2634.
14. Guan, Z.; Tang, A.; Lv, P.; Liu, Z.; Li, X.; Tan, Z.; Hayat, T.; Alsaedi, A.; Yang, C.; Teng, F. New Insights into the Formation and Color-Tunable Optical Properties of Multinary Cu-In-Zn-based Chalcogenide Semiconductor Nanocrystals. Adv. Opt. Mater. 2018, 6, 1701389.
15. Chetty, S.S.; Praneetha, S.; Murugan, A.V.; Govarthanan, K.; Verma, R.S. Human Umbilical Cord Wharton's Jelly-Derived Mesenchymal Stem Cells Labeled with Mn2+ and Gd3+ Co-Doped CuInS2–ZnS Nanocrystals for Multimodality Imaging in a Tumor Mice Model. ACS Appl. Mater. Interfaces 2020, 12, 3415–3429.
16. Ueng, H.Y.; Hwang, H.L. The defect structure of CuInS2. Part I: Intrinsic defects. J. Phys. Chem. Solids 1989, 50, 1297–1305.
17. Huang, L.; Publicover, N.G.; Hunter, K.W.; Ahmadiantehrani, M.; de Bettencourt-Dias, A.; Bell, T.W.; Zhu, X. Cadmium and Zinc Alloyed Cu-In-S Nanocrystals and Their Optical Properties. J. Nanopart. Res. 2013, 15, 2056.
18. Zang, H.; Li, H.; Makarov, N.S.; Velizhanin, K.A.; Wu, K.; Park, Y.S.; Klimov, V.I. ThickSshell CuInS2/ZnS Quantum Dots with Suppressed "Blinking" and Narrow Single-Particle Emission Line Widths. Nano Lett. 2017, 17, 1787–1795.
19. Yarema, O.; Yarema, M.; Wood, V. Tuning the Composition of Multicomponent Semiconductor Nanocrystals: The Case of I–III–VI Materials. Chem. Mater. 2018, 30, 1446–1461.
20. Pradhan, N. Red-Tuned Mn d-d Emission in Doped Semiconductor Nanocrystals. ChemPhysChem 2015, 17, 1087–1094.
21. Manna, G.; Jana, S.; Bose, R.; Pradhan, N. Mn-Doped Multinary CIZS and AIZS Nanocrystals. J. Phys. Chem. Lett. 2012, 3, 2528–2534.
22. Tang, X.; Zu, Z.; Bian, L.; Du, J.; Chen, W.; Zeng, X.; Wen, M.; Zang, Z.; Xue, J. Synthesis of Mn Doping Ag–In–Zn–S Nanoparticles and Their Photoluminescence Properties. Mater. Des. 2016, 91, 256–261.
23. Liu, Q.; Deng, R.; Ji, X.; Pan, D. Alloyed Mn–Cu–In–S Nanocrystals: A New Type of Diluted Magnetic Semiconductor Quantum Dots. Nanotechnology 2012, 23, 255706.
24. Cao, S.; Li, C.; Wang, L.; Shang, M.; Wei, G.; Zheng, J.; Yang, W. Long-Lived and Well-Resolved Mn2+ Ion Emissions in CuInS-ZnS Quantum Dots. Sci. Rep. 2014, 4, 7510.

25. Cao, S.; Zhao, J.; Yang, W.; Li, C.; Zheng, J. Mn2+-doped Zn–In–S Quantum Dots with Tunable Bandgaps and High Photoluminescence Properties. J. Mater. Chem. C 2015, 3, 8844–8851.
26. Peng, L.; Li, D.; Zhang, Z.; Huang, K.; Zhang, Y.; Shi, Z.; Xie, R.; Yang, W. Large-scale synthesis of single-source, thermally stable, and dual-emissive Mn-doped Zn–Cu–In–S nanocrystals for bright white light-emitting diodes. Nano Res. 2015, 8, 3316–3331.
27. Jo, D.-Y.; Kim, D.; Kim, J.-H.; Chae, H.; Seo, H.J.; Do, Y.R.; Yang, H. Tunable White Fluorescent Copper Gallium Sulfide Quantum Dots Enabled by Mn Doping. ACS Appl. Mater. Interfaces 2016, 8, 12291–12297.
28. Kim, J.-H.; Kim, B.-Y.; Yang, H. Synthesis of Mn-doped CuGaS2 quantum dots and their application as single downconverters for high-color rendering solid-state lighting devices. Opt. Mater. Express 2018, 8, 221–230.
29. Kim, J.H.; Kim, K.H.; Yoon, S.Y.; Kim, Y.; Lee, S.H.; Kim, H.S.; Yang, H. Tunable Emission of Bluish Zn–Cu–Ga–S Quantum Dots by Mn Doping and Their Electroluminescence. ACS Appl. Mater. Interfaces 2019, 11, 8250–8257.
30. Gallian, B.; Dong, G.; Zhu, X. A compact time-gated instrument for QDs with low excitation energy and millisecond fluorescence lifetime as signal reporters, and its detection application. Rev. Sci. Instrum. 2019, 90, 104701.
31. Sperling, R.A.; Parak, W.J. Surface Modification, Functionalization and Bioconjugation of Colloidal Inorganic Nanoparticles. Philos. Trans. R. Soc. A 2010, 368, 1333.